Earth and Planetary Science Letters, 116 (1993) 63–80
Elsevier Science Publishers B.V., Amsterdam

[DT]

Interpretation and tectonic implications of cooling histories: An example from the Black Mountains, Death Valley extended terrane, California

Daniel K. Holm [a,1] and Roy K. Dokka [b]

[a] *Department of Earth and Planetary Sciences, Harvard University, Cambridge, MA 02138, USA*
[b] *Department of Geology and Geophysics, Louisiana State University, Baton Rouge, LA 70803-4101, USA*

Received May 30, 1992; revision accepted January 19, 1993

ABSTRACT

In the Death Valley extended terrane of California, the Black Mountains have long been considered unique because they largely lack the miogeoclinal cover rocks characteristic of the surrounding ranges. Fission-track ages presented here are combined with published $^{40}Ar/^{39}Ar$ ages and used to construct cooling path envelopes for samples of Precambrian crystalline basement and Miocene plutonic rocks collected across the entire range. The cooling history reconstructions are used to differentiate between contrasting Miocene unroofing histories proposed for this range. Apatite and zircon fission-track ages from the southeastern portion of the range suggest unroofing occurred there at ~ 13–8.5 Ma from temperatures well below 300°C. Cooling age data from the central Black Mountains indicate major unroofing at 8.5–6.0 Ma from temperatures greater than 300°C. Old cooling ages from directly beneath the highly extended Amargosa chaos rocks are consistent with the chaos rocks being part of an allochthonous slice that was tectonically transported from high crustal levels onto deeper crustal levels.

Scenarios for the Miocene unroofing history of this range rely heavily on interpretations of the depth of emplacement of Miocene plutons in the core of the range. Thermochronologic and geobarometric data and thermal modeling of intrusion cooling suggest emplacement of an 11.6 Ma pluton into the crystalline core at a depth of 10–15 km. Both the cooling-age data and considerations of the local geology seem to preclude an unroofing history dominated by erosion of the overlying miogeoclinal section. The morphology of the cooling path envelopes constructed here are similar to those constructed for detachment fault terranes. The data are most consistent with unroofing involving tectonic denudation (10–15 km) along a single, westerly dipping detachment zone. Diachronous rapid cooling from southeast to northwest within the range is interpreted as a result of the lower plate undergoing flexural deformation as it pulls out from underneath a relatively rigid, scoop-shaped hanging wall block (the 'rolling-hinge' model). Migration of unroofing and tilting within the range mimics the overall east to west sequential tilting and unroofing of range blocks in the Death Valley extended terrane. Similar thermochronologic evidence for sequential range-scale tilting has been obtained from the Lake Mead extended region, suggesting that this style of extension might provide an explanation for strongly extended domains in the Basin and Range Province.

1. Introduction

Determining the time, amount, and nature of unroofing of rocks is fundamental to an understanding of the processes of lithospheric deformation. Erosion and tectonic denudation are both processes which result in the unroofing of rocks from depth. As these processes have very different implications for the nature of crustal deformation, a major challenge lies in determining how unroofing is partitioned between them. During the past decade, the construction of temperature–time histories has become an increasingly important technique for assessing the nature of unroofing. Cooling ages provide one method for differentiating between fast, tectonically driven unroofing and slower, erosion-dominated unroofing. By combining $^{40}Ar/^{39}Ar$ and fission-track age

[1] Now at: Department of Geology, Kent State University, Kent, OH 44242, USA

TABLE 1

Mineral closure temperatures used in this study

Mineral	Technique[40]	Closure temperature	Reference
Hornblende	$Ar/^{39}Ar^{40}$	500 ± 25°C	[1]
Muscovite	$Ar/^{39}Ar^{40}$	350 ± 25°C	[1]
Biotite	$Ar/^{39}Ar$	300 ± 25°C	[1]
Sphene	Fission track	285 ± 25°C	[2]
Zircon	Fission track	205 ± 25°C	[3]
Apatite	Fission track	120 ± 25°C	[4]

determinations on a variety of minerals from the same area (or hand sample), one can constrain a large portion of the cooling history of an area (or rock) because of differences in closure temperatures between mineral systems (Table 1). Rapid cooling, as suggested by concordant mineral ages, can be a strong indication of tectonic unroofing. In contrast, rocks uplifted during erosion-dominated unroofing will have relatively slow cooling rates so that different minerals from the same rock will give discordant ages.

Relationships in the Death Valley region, California, have had a great influence on developing ideas on the nature of continental extension. In spite of the great amount and variety of research in this fascinating region, many interpretations of its geologic history conflict. One such controversy pertains to the unroofing history of the Black Mountains on the east side of Death Valley (Fig. 1). This mountain range has long been considered peculiar because it largely lacks the miogeoclinal sedimentary cover rocks characteristic of the surrounding ranges [5]. Contrasting viewpoints advocate differing amounts, times and rates of Miocene unroofing of this range block associated with very different models for the tectonic evolution of this region. These models also differ in their estimate of the dip of normal faults responsible for unroofing and in the overall amount of extension that has occurred in the Death Valley region. In an attempt to address this controversy and also to better understand both the timing and amount of unroofing of this range block, we have used fission track thermochronology to constrain the low-temperature history of this range. When combined with previously reported $^{40}Ar/^{39}Ar$ age determinations, these data provide important constraints on the unroofing history of this range and on the tectonic history of the Death Valley region in general.

2. Geology of the Black Mountains

The Black Mountains are a NW-trending range centrally located in the Death Valley extensional terrane, between the relatively unextended Spring Mountains block to the east and the Sierra Nevada to the west. In the southeast, Precambrian crystalline basement rocks are nonconformably overlain by Late Precambrian and younger strata that dip moderately to steeply to the east (Fig. 2). Approximately 15–20 km to the northwest, in the middle of the range, these same strata are complexly faulted and extended, forming the Amargosa chaos [6]. Northwest of the exposures of the chaos, variably faulted and ductilely sheared Miocene plutons are intruded into amphibolite facies Eocambrian metasedimentary rocks and middle Proterozoic crystalline schist and gneiss [7,8]. The oldest pluton (the Willow Spring Pluton) is a sill-shaped, intermediate to mafic composition batholith which has yielded a U/Pb zircon age of 11.6 ± 0.2 Ma [9]. A large silicic complex intrusive into the Willow Spring

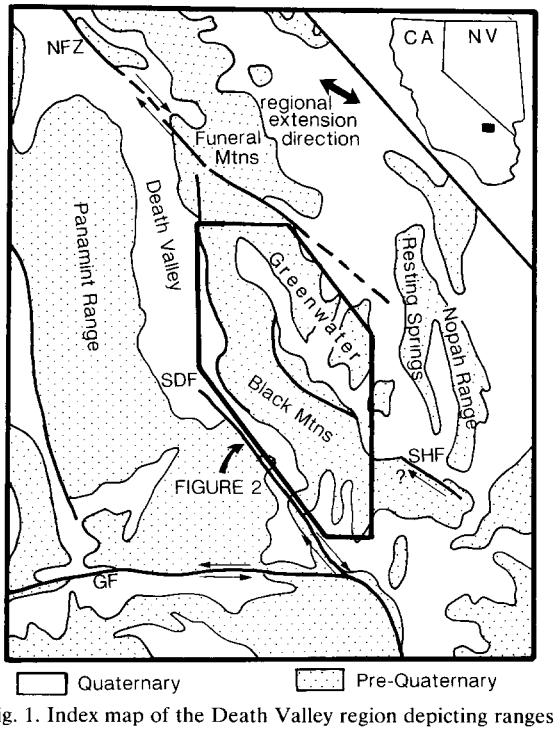

Fig. 1. Index map of the Death Valley region depicting ranges and major faults. *NFZ* = Northern Death Valley–Furnace Creek fault zone; *SDF* = Southern Death Valley fault; *SHF* = Sheephead fault; *GF* = Garlock fault.

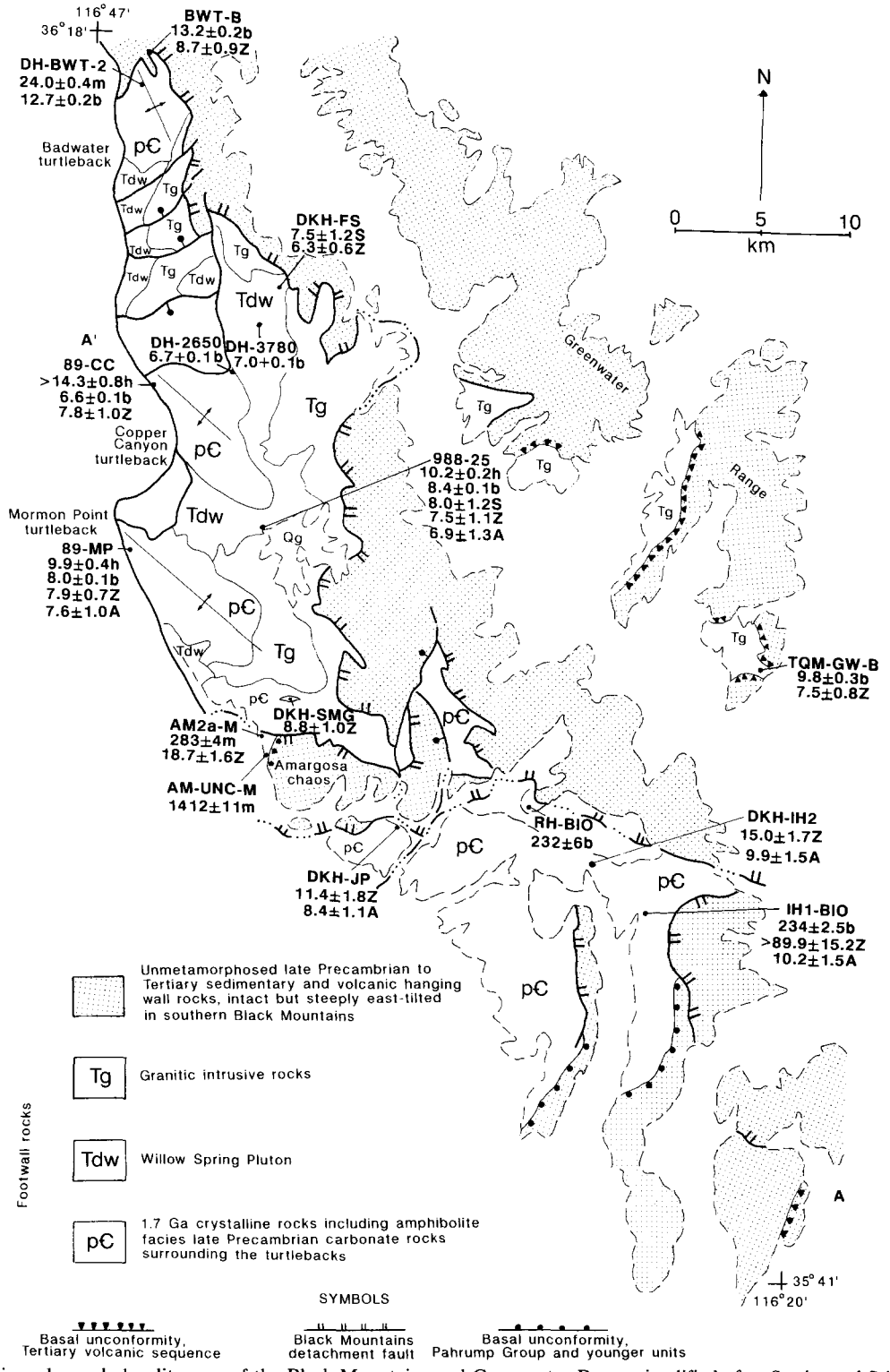

Fig. 2. Geologic and sample locality map of the Black Mountains and Greenwater Range simplified after Streitz and Stinson [71] and Holm and Wernicke [28]. Mineral cooling age data are in Ma. h = hornblende; m = muscovite; b = biotite; S = sphene; Z = zircon; A = apatite. Errors are given at one standard deviation.

Pluton yielded two $^{40}Ar/^{39}Ar$ hornblende ages of ~ 8.7 Ma [10]. On the eastern side of Death Valley, the Precambrian rocks are folded into NW-plunging antiforms known as the Death Valley 'turtlebacks'. Whereas the exposure of the antiforms was first related to Tertiary extensional tectonism [11], the folding of these rocks has recently been suggested as being Miocene in age or younger [12,13].

The northern and eastern portions of the crystalline complex are overlain by variably faulted volcanic strata of post-10 Ma age [14]. The western portion of the Black Mountains contains two isolated and fault-bounded basin deposits of uppermost Miocene to Quaternary age which appear to record the last stages of unroofing of the crystalline core of the range [8,12,15]. The occurrence of clasts of the Miocene plutonic rocks in one of these basins indicates they were exposed by ~ 5 Ma [9]. Sedimentary rocks of the Late Precambrian/Paleozoic miogeoclinal section, which make up the majority of the surrounding ranges (the Panamint Range, Funeral Mountains, and Resting Springs/Nopah Ranges), are largely absent in the Black Mountains.

3. Proposed unroofing histories

The relative scarcity of miogeoclinal rocks in the Black Mountains (compared to the surrounding ranges) has been explained by two very different models for the unroofing history of the range. Erosion and tectonic denudation are end-member processes responsible for unroofing, and it is obvious that both of these processes occur simultaneously. While Wright and Troxel [16] and Wright et al. [11] clearly showed that tectonic denudation played a role in the unroofing of the Black Mountains, more recent investigations (particularly on Neogene basin deposits surrounding the Black Mountains) have led them and their coworkers to emphasize that erosion, perhaps, also played an important role in the unroofing history of the Black Mountains [17–19]. Wright et al. [20,21] envisage the Black Mountains as having formed in a pull-apart setting where Neogene faulting, volcanism and shallow intrusion are controlled by a right-step across two major right-lateral strike-slip faults (the Sheephead and Furnace Creek fault zones, Fig. 1). Accordingly, the NW-striking strike-slip faults and the intervening N- to NE-striking, steep to moderate normal faults (not shown in Fig. 1) are the principal expressions of crustal failure [20,22–24]. Where the latter are shallow and closely spaced, they form the Amargosa chaos. Wright et al. [20,25] attribute limited movement on the Amargosa fault (and development of the overlying chaos) as genetically related to eastward tilting of the Resting Spring Range at 10–11 Ma. Whereas slices of the Proterozoic–Paleozoic cover rocks exist within portions of the chaos, Wright and Troxel [26] also mapped areas where these rocks are exposed over nearly their full thickness and appear depositional on basement. Because clasts of Proterozoic–Paleozoic rocks occur in inverted succession within Neogene basin deposits surrounding the Black Mountains, Cemen and Wright [19] and Prave and Wright [17,18] argued that Neogene denudation of the Black Mountains was accomplished at least locally by erosion.

In contrast to the above scenario, some workers [5,12] suggest that the sedimentary package comprising the Panamint Range (Fig. 1) was originally positioned above the Black Mountains. Stewart [5] proposed that the Panamint Range was tectonically removed from the western part of the Black Mountains during Neogene extension. Holm and Wernicke [28] hypothesized, on the basis of geobarometric, metamorphic and deformational features, that the Black Mountains block represents a pre-extensional section of the crust unroofed along a major westerly dipping detachment zone. This hypothesis is consistent with reconstructions of Neogene deformation requiring large amounts of extension in the southern Great Basin [29,30]. According to the detachment model, the rocks of the Amargosa chaos represent a stranded portion of the hanging wall block that was translated 15–20 km northwestward from an initial position in the southeasternmost portion of the range. The detachment is inferred to have locally cut into crystalline basement, leaving localized areas where the sedimentary chaos rocks are nonconformable on slivers of detached basement (i.e., the Ashford Canyon region, [28]).

Both scenarios for the Miocene unroofing history of this range block rely heavily on interpreta-

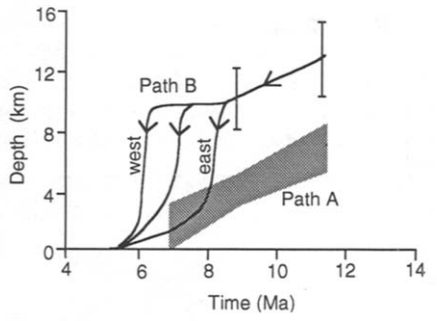

Fig. 3. Reconstruction of proposed unroofing histories for the crystalline rocks of the Black Mountains core. Denudation dominated by erosion and accompanied by high-angle normal faulting (path A) after Wright et al. [20]. Denudation expected for westerly directed detachment faulting (path B) after Holm and Wernicke [28] and Holm et al. [10]. Error bars for path B represent depth estimates for emplacement of two plutonic complexes after Holm et al. [10].

tions of the depth of emplacement of Miocene plutons which have intruded the Precambrian basement and metasedimentary rocks forming the antiforms. Geobarometric results (using the Al-in-hornblende calibration of Johnson and Rutherford, [31]) indicate a lower bound on the depth estimate for crystallization of the 11.6 Ma Willow Spring Pluton at 9.5–12.5 km and a depth estimate of 10.0 ± 1.8 km for the 8.7 Ma Smith Mountain Granite Complex [10]. (Greater depth estimates are obtained if the equation of Hollister et al. [32] is used.) In contrast, Wright et al. [20] prefer a much shallower emplacement depth for both of these intrusions (7 ± 1 km for the Willow Spring Pluton and 6 km for the younger granite). Also using the Al-in-hornblende geobarometer, they reported paleopressures for the granite of 1.7 kbar. Their results are difficult to evaluate, however, as they did not present the data in their report. However, we point out that their result is inconsistent with the requirement that pressure be above ~ 2 kbar in order to reliably apply the barometer, as the Al content of hornblende may become temperature- (as well as pressure-) sensitive below 2 kbar [32].

The proposed unroofing histories are summarized in Table 2 and are depicted graphically in Fig. 3. They differ significantly in both the amount and the rate of unroofing responsible for exposure of the antiforms and the Miocene plutons surrounding them. The pull-apart model (path A of Fig. 3) proposes a relatively constant and moderate unroofing rate from an initial depth no greater than 7 ± 1 km. The detachment fault model (path B of Fig. 3) proposes an initial slow to moderate unroofing rate at midcrustal depths prior to ~ 8.5 Ma followed by diachronous rapid unroofing from depths of 8–12 km (Table 2). As will be discussed below, determination of which, or if either, of these two scenarios is consonant with the data is important in order to understand the kinematics of crustal extension in this region.

4. Sampling and analytical methods

A total of eighteen fission-track age determinations were obtained from eleven samples collected across the length of the mountain range (Fig. 2). Wherever possible, fission-track mineral separates (apatite, zircon and sphene) were obtained from samples already dated by the $^{40}Ar/^{39}Ar$ method in order to reconstruct the most

TABLE 2

Summary of proposed unroofing histories

A. Pull-apart model (after [20]; depicted as path A in Fig. 3)

(1) 11.6 Ma Willow Spring Pluton emplaced at no greater than 7 ± 1 km.
(2) Erosional and tectonic denudation (by high-angle normal faulting) begins soon after emplacement.
(3) ~ 9 Ma silicic plutons intrude the Willow Spring Pluton at < 5 km.
(4) Erosional and tectonic denudation continues such that by 7 Ma the upper part of the Willow Spring Pluton has been exposed at the earth's surface.

B. Detachment model (after [28] and [10]; depicted as path B in Fig. 3)

(1) 11.6 Ma Willow Spring Pluton emplaced at a depth of 10–15 km.
(2) ~ 9 Ma silicic plutons intrude the Willow Spring Pluton at ~ 8–12 km.
(3) Tectonic denudation by westerly directed detachment faulting results in progressive rapid unroofing between ~ 8.5 and 6.0 Ma.
(4) Willow Spring Pluton exposed by 5.0 Ma.

TABLE 3

Fission track data from the Black Mountains, Death Valley, California

Field name (Lab #)	Mineral Dated	Spontaneous Track Density, tracks/cm^2 (tracks counted)	Induced Track Density, tracks/cm^2 (tracks counted)	Standard Track Density, tracks/cm^2 (tracks counted)	Grains Counted	Chi Squared Probability[$]	Correlation Coefficient[*]	Age (Ma)[#]	±1σ (Ma)
988–25 (900004)	sphene	8.27E+04 (62)	3.27E+05 (245)	1.90E +05 (2026)	8	0.748	0.968	8.0	1.2
DKH-FS (900007)	sphene	6.80E+06 (51)	2.87E+05 (215)	1.89E+05 (2026)	8	0.452	0.700	7.5	1.2
DKH-SMG (900002)	zircon	5.53E+05 (109)	1.99E+05 (392)	1.89E+05 (2026)	7	0.468	0.970	8.8	1.0
988-25 (900003)	zircon	2.44E+05 (62)	1.02E+06 (260)	1.88E+05 (2026)	8	1.993	0.831	7.5	1.1
TQM-GW-B (900029)	zircon	4.95E+05 (103)	2.03E+06 (423)	1.84E+05 (2026)	8	0.555	0.992	7.5	0.8
DKH-FS (900006)	zircon	5.66E+05 (128)	2.81E+06 (636)	1.88E+05 (2026)	8	0.510	0.980	6.3	0.6
AM2a–M (900028)	zircon	1.56E+05 (222)	2.58E+06 (366)	1.84E+05 (2026)	11	4.916	0.983	18.7	1.6
DKH–JP (900010)	zircon	5.70E+05 (57)	1.57E+06 (157)	1.87E+05 (2026)	6	0.588	0.837	11.4	1.8
89-MP (900011)	zircon	1.07E+06 (155)	4.21E+06 (611)	1.87E+05 (2026)	8	1.437	0.994	7.9	0.7
BWT-B (900012)	zircon	1.96E+06 (131)	6.96E+06 (466)	1.86E+05 (2026)	7	0.441	0.989	8.7	0.9
DKH-IH2 (900014)	zircon	9.60E+05 (120)	1.98E+06 (248)	1.86E+05 (2026)	8	1.438	0.939	15.0	1.7
IH1-BIO (900021)	zircon	9.33E+06 (140)	3.20E+06 (48)	1.85E+05 (2026)	2	0.173		89.9	15.2
89-CC (900023)	zircon	3.96E+05 (84)	1.57E+06 (332)	1.85E+05 (2026)	8	0.664	0.977	7.8	1.0
DKH-JP (900013)	apatite	9.43E+04 (66)	2.43E+06 (1698)	4.03E+04 (2014)	7	0.292	0.994	8.4	1.1
988-25 (900017)	apatite	1.99E+04 (29)	6.18E+05 (899)	4.02E+04 (2014)	15	1.783	0.597	6.9	1.3
IH1–BIO (900019)	apatite	2.59E+04 (51)	5.42E+05 (1067)	3.99E+04 (2014)	20	2.400	0.885	10.2	1.5
89–MP (900020)	apatite	4.83E+04 (58)	1.35E+06 (1625)	3.97E+04 (2014)	12	1.822	0.851	7.6	1.0
DKH-IH2 (900022)	apatite	3.00E+04 (48)	6.39E+05 (1023)	3.96E+04 (2014)	16	3.560	0.700	9.9	1.5

[$] Probability of obtaining χ^2 value [28] for n degrees of freedom (n is number of grains minus 1).

[*] Comparison between individual crystal track counts.

[#] Calculated following to [65] using zeta values of 335 and 10,626 for zircon–sphene and apatite, respectively.

complete cooling history possible for individual samples. This was done to avoid the undesirable situation of having the higher temperature history ($\sim$ 300°–500°C) constrained for some samples and the lower temperature history ($\sim$ 285°– < 100°C) constrained for others, thus making interpretation of the cooling history for the range block more difficult. Mineral separates, in the size range 62–250 μm, were obtained using a concentrating table, heavy liquids and a magnetic separator at the Louisiana State University fission-track laboratory.

Zircons and sphenes were embedded in translucent FEP Teflon™ on a hot plate at $\sim$ 350°C, ground with 600 grade silicon carbide paper in water and polished with diamond pow-

TABLE 4

Summary of Black Mountains cooling-age data

Sample	Rock type	Locality	Mineral	Elevation	Age ±2σ (Ma)
		Southeastern Black Mountains			
IH1–BIO	pC basement	116°25.6' W, 35°52.5' N	biotite	1,119	234.3 ± 2.5*
			zircon		>89.9 ± 30.4
			apatite		10.2 ± 3.0
DKH–IH2	pC basement	116°26.3' W, 35°53.7' N	zircon	985	15.0 ± 3.4
			apatite		9.9 ± 3.0
RH–BIO	pC basement	116°30.0' W, 35°55.0' N	biotite	671	232.3 ± 5.9*
DKH–JP	pC basement	116°34.4' W, 35°54.5' N	zircon	366	11.4 ± 3.6
			apatite		8.4 ± 2.2
		Ashford Canyon			
AM-UNC-M	pC basement	116°39.6' W, 35°56.4' N	muscovite	195	1411.6 ± 10.7*
AM2a–M	pC basement	116°40.2' W, 35°57.5' N	muscovite	317	283.2 ± 4.1*
			zircon		18.7 ± 3.2
		Central Black Mountains Core			
DKH–FS	gabbro-diorite	116°40.0' W, 36°10.2' N	sphene	1,686	7.5 ± 2.4
			zircon		6.3 ± 1.2
DKH–SMG	granite	116°39.0' W, 35°58.3' N	zircon	610	8.8 ± 2.0
89–CC	pC basement	116°44.1' W, 36°06.6' N	hornblende	–60	>14.3 ± 0.8*
			biotite		6.6 ± 0.1*
			zircon		7.8 ± 2.0
988–25	gabbro-diorite	116°40.4' W, 36°03.1' N	hornblende	975	10.2 ± 0.2*
			biotite		8.4 ± 0.1*
			sphene		8.0 ± 2.4
			zircon		7.5 ± 2.2
			apatite		6.9 ± 2.6
89–MP	pC basement	116°45.1' W, 36°02.0' N	hornblende	61	9.9 ± 0.4*
			biotite		8.0 ± 0.14*
			zircon		7.9 ± 1.4
			apatite		7.6 ± 2.0
DH–3780	gabbro-diorite	116°40.4' W, 36°08.0' N	biotite	1,152	7.0 ± 0.1*
DH–2650	gabbro-diorite	116°41.9' W, 36°07.5' N	biotite	808	6.7 ± 0.1*
		Northern Black Mountains			
BWT–B	pC basement	116°45.6' W, 36°17.1' N	biotite	265	13.2 ± 0.2*
			zircon		8.7 ± 1.8
DH–BWT–2	pC basement	116°45.0' W, 36°16.3' N	muscovite	732	24.0 ± 0.4*
			biotite		12.7 ± 0.2*
		Greenwater Range			
TQM-GW-B	granite	116°21.8' W, 35°59.9' N	biotite	902	9.8 ± 0.3*
			zircon		7.5 ± 1.6

* Data obtained by the $^{40}Ar/^{39}Ar$ method and discussed in [10]. Elevations in meters; pC = Precambrian.

der. They were then etched in molten KOH–NaOH eutectic at ~ 220°C for times varying between 13 and 70 h. Apatite grains were mounted in epoxy on microscope slides, ground using 400 and 600 grade silicon carbide paper and polished with 6 μm and 1 μm diamond compound. The apatites were then etched in 5*M* HNO_3 for 20–30 s at room temperature. After etching all mounts were cleaned in detergent, alcohol and distilled water.

All samples were dated utilizing the external detector method [33], using analytical methods described in Dokka et al. [4]. Mounts were placed in intimate contact with low-U muscovite external detectors. Each batch of mounts for irradiation was stacked vertically between two pieces of uranium dosimeter glass which had been prepared in similar fashion. National Bureau of Standards dosimeter glasses 962 and 963a coupled with muscovite detectors were used with (i) zircons and sphene and (ii) apatite samples, respectively. These dosimeters were calibrated against the Fish Canyon zircon and apatite using an age of 27.88 Ma. Samples were irradiated at the U.S. Geological Survey Triga Reactor in Denver, Colorado.

After irradiation, the muscovite external detectors were detached and etched in 48% HF for 20 min at room temperature. Counting of tracks was greatly facilitated by the use of a microcomputer-controlled automatic stage. Fission-track ages were determined using the zeta calibration technique, which eliminates the need for absolute thermal neutron dosimetry and selection of a value for the spontaneous fission decay constant of ^{238}U. Analytical data and results are given in Table 3. Statistical uncertainty for all age determinations is expressed as two standard deviations and was calculated following Galbraith [34]. So little is known about the annealing characteristics of sphene and zircon that track-length measurements are not done on them. In this study, because of the extremely low spontaneous track density in apatite grains, confined track-length measurements were not possible.

5. Results of fission-track dating

The results of this study are discussed with respect to individual mineral types (sphene, zircon and apatite). Specific localities, elevations, ages, etc. from this study and from a prior $^{40}Ar/^{39}Ar$ study are summarized in Table 4. Table 1 shows the closure temperatures assumed for this study in order to interpret the data. Closure temperature is cooling-rate dependent [35], with higher closure temperatures associated with rapid cooling. Many of the fission-track cooling ages presented here for individual samples are concordant (within 2σ error) and some are even concordant with higher temperature $^{40}Ar/^{39}Ar$ cooling ages, suggesting rapid cooling. Therefore, we have chosen published fission-track closure temperature values obtained from other studies in rapidly cooling regions.

Sphene: The mineral sphene is abundant in the Willow Spring Pluton [9]. Two sphene separates were obtained from samples of the batholith in the central portion of the Black Mountains crystalline terrane (Fig. 2). A sphene fission-track age of 8.0 ± 2.4 Ma from sample 988–25 near Willow Spring is concordant with a biotite $^{40}Ar/^{39}Ar$ age of 8.4 ± 0.1 Ma obtained on the same sample (Table 4). Sphene from sample DKH–FS located ~ 13 km north of Willow Spring yielded an age of 7.5 ± 2.4 Ma. These sphene ages are identical within error of one another and suggest that the crystalline core of the range cooled through ~ 285°C prior to ~ 5.5 Ma.

Zircon: Ten zircon separates were obtained from Miocene intrusions and Precambrian basement throughout the Black Mountains. Zircon fission-track ages decrease towards the northwest, with the exception of sample AM2a–M at Ashford Canyon, which yielded an age of 18.7 ± 3.2 Ma. The oldest zircon age was obtained from IH1–BIO in the southeastern Black Mountains, a sample located ~ 3.5 km structurally beneath the Precambrian nonconformity (Upper Precambrian Pahrump Group strata depositional on 1.7 Ga basement). Zircon grains from this sample often contained spontaneous tracks with such a high density that they could not be distinguished from one another for counting purposes. Two grains with a relatively low density of tracks were counted in an effort to establish a likely minimum age (considering the probability of missing tracks in counting). These gave grain ages of 95 and 82 Ma, giving a pool age of 89.9 ± 30.4 Ma. Whereas this age lacks statistical confidence and precision, we consider it likely to be a minimum age for this

sample. This same sample yielded a biotite $^{40}Ar/^{39}Ar$ total gas age of 234.3 ± 2.5 Ma (Table 3).

Zircon fission-track ages decrease to the northwest of sample IH1–BIO. Three kilometers north of sample IH1–BIO, zircons in Precambrian basement yielded a fission-track age of 15.0 ± 3.4 Ma (sample DKH–IH2). A zircon fission-track age of 11.4 ± 3.6 Ma (sample DKH–JP) was obtained from Precambrian basement gneiss near Jubilee Pass northwest of sample DKH–IH2. North of Ashford Canyon, mean zircon fission-track ages in the central Black Mountains core from both Miocene intrusions and Precambrian basement range from 8.7 to 6.3 Ma (Table 4). All of the ages from the crystalline core are identical (within error) to one another, with overlap at 7.0–7.5 Ma. The zircon ages are also within error of the sphene ages discussed above, suggesting that the crystalline core of the Black Mountains cooled rapidly.

Apatite: Apatite ages from the Black Mountains were difficult to obtain due to the presence of numerous inclusions in the majority of apatite grains. Although ten of the eleven samples contained enough apatite to yield a mineral separate for dating, only five separates had grains that were suitable for dating. Three apatite ages were obtained from Precambrian basement in the southern Black Mountains (samples IH1–BIO, DKH–IH2 and DKH–JP) and two from the central crystalline core of the range (samples 988–25 and 89–MP). Due to the low precision in age determinations for extremely young samples using this technique, all of the apatite ages from the Black Mountains are concordant (within 2σ error), with overlap in the time span 7.5–9.7 Ma (Table 3). The lower age limits from apatite separates in the core of the range indicate that this portion of the range cooled through ~ 100°C by at least 5.5–4.5 Ma. This is consistent with sedimentologic evidence that indicates exposure of rocks making up the turtleback surfaces by ~ 5 Ma [3,4,7].

6. Interpretation of cooling histories

A frequently utilized approach for reconstructing the cooling history of a rock is to use the age and closure temperature (and their accompanying uncertainties) of several different mineral thermochronometers, each one constraining a different portion of the cooling path. Our cooling history reconstruction of individual samples throughout the Black Mountains is depicted in Fig. 4 and is based on fission track ages, $^{40}Ar/^{39}Ar$ ages [10], and time of first appearance of clasts in hanging wall sedimentary basins. We treat the cooling paths as fields of time–temperature space rather than as lines because it is important to account for the uncertainty of the age determinations and closure temperatures. This time–temperature space is referred to as the *cooling path envelope* [4,36]. In constructing an envelope, we assume monotonically decreasing temperatures between cooling ages. The envelope contains all possible cooling histories that the particular sample could have experienced during unroofing. There is no *a priori* reason to assume that rocks cool linearly between regions constrained by the age data. After quantitatively reconstructing the cooling envelopes, we then qualitatively assess the most likely cooling path experienced by each rock using knowledge of the regional and local geology, distribution of ages across the range, etc. We have depicted this 'preferred' path as a dashed line within each cooling path envelope (Fig. 4).

Southeastern Black Mountains: Figures 4a and b are cooling path envelopes constructed from samples in the southeastern portion of the Black Mountains. The temperature–age data for Fig. 4a (Ibex Hills) are from a single sample (IH1–BIO) whereas Fig. 4b (Jubilee Pass) combines zircon and apatite fission-track ages from sample DKH–JP with the biotite $^{40}Ar/^{39}Ar$ age from sample RH–BIO. Biotites from this region yield total gas $^{40}Ar/^{39}Ar$ ages of ~ 230–235 Ma [9]. One interpretation of these data is that the ages represent simple slow cooling through ~ 300°C associated with slow unroofing at 230–235 Ma. However, considering their proximity to unmetamorphosed Precambrian strata, it seems likely that these rocks have not been buried to great depths since deposition of the overlying Upper Precambrian strata. We propose an alternative explanation, therefore: that these biotite ages might record an Early Triassic thermal resetting event.

Permian to Triassic plutonism has long been recognized in the northern and southern parts of the Cordilleran orogen. Southeast of the Black

Mountains, plutonism of apparently Late Triassic age is indicated from K-Ar hornblende ages in the Clark Mountains [37,38]. To the northwest, age determinations in the Cottonwood Mountains of northern Death Valley [39] indicate post-thrusting intrusions of Permo-Triassic age which give mid-Late Triassic muscovite and biotite cooling ages similar to the ages obtained in the southern Black Mountains. Whereas these three areas are currently over 210 km apart, reconstructions of Tertiary extension restore them into a narrow northerly trending transect (Fig. 5, [29,40,41]). The apparent proximity of Permian–Triassic intrusions to the southern Black Mountains prior to Tertiary extension suggests that the 230–235 Ma $^{40}Ar/^{39}Ar$ ages might represent thermal resetting due to intrusion.

The minimum 90 Ma zircon age and the middle Miocene apatite age for sample IH1-BIO indicates that this sample was between ~200°C and 100°C before the onset of regional Tertiary extension and cooled through 100°C during un-

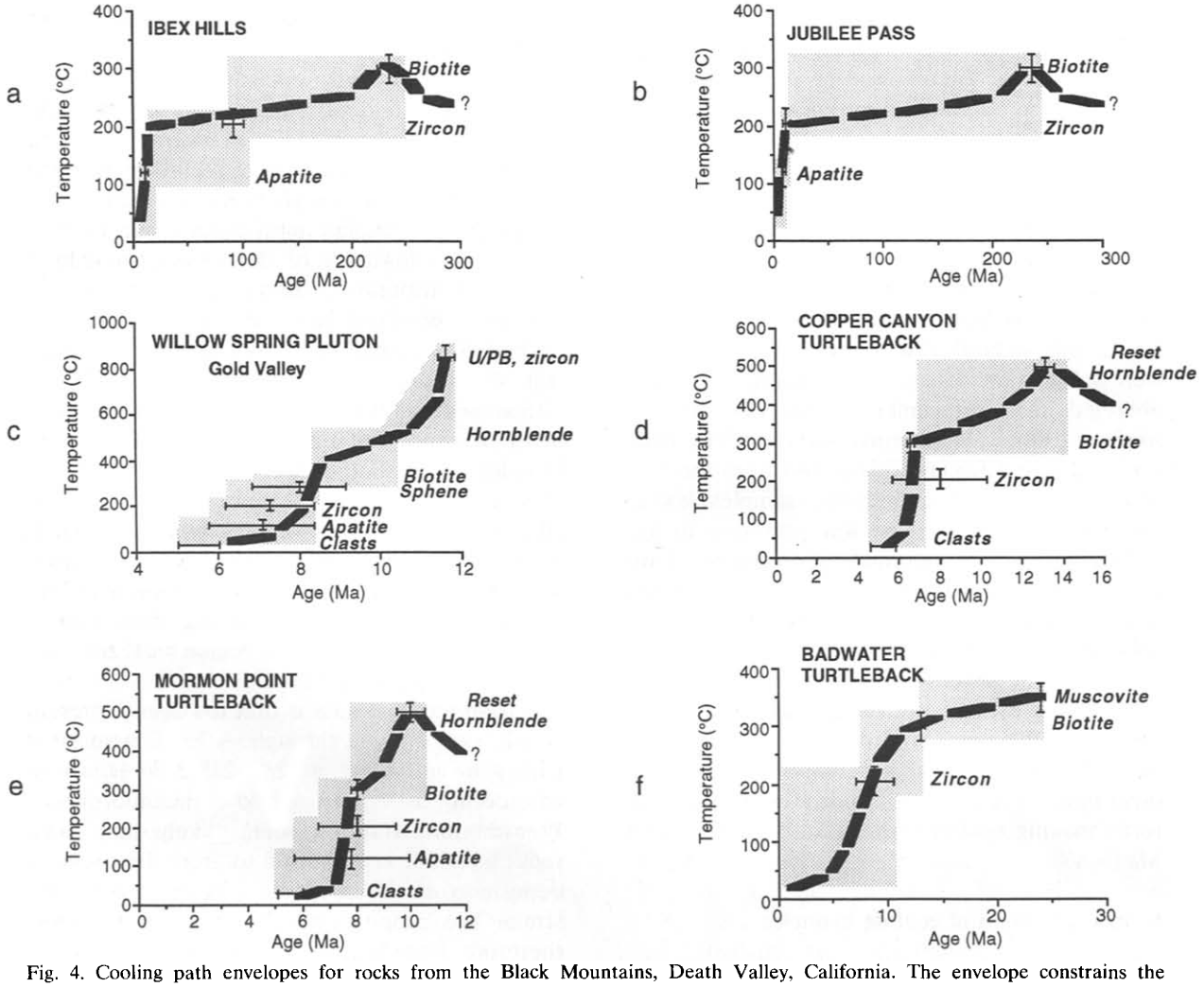

Fig. 4. Cooling path envelopes for rocks from the Black Mountains, Death Valley, California. The envelope constrains the time-temperature space where cooling paths can exist. The geometry of the envelope (shaded region) is based on closure temperature–apparent age (plus precision estimate) relationships of fission track (apatite, zircon and sphene) and $^{40}Ar/^{39}Ar$ (biotite, muscovite and hornblende) thermochronometers. Dashed lines represent what we consider to be the most likely cooling path. See text for discussion.

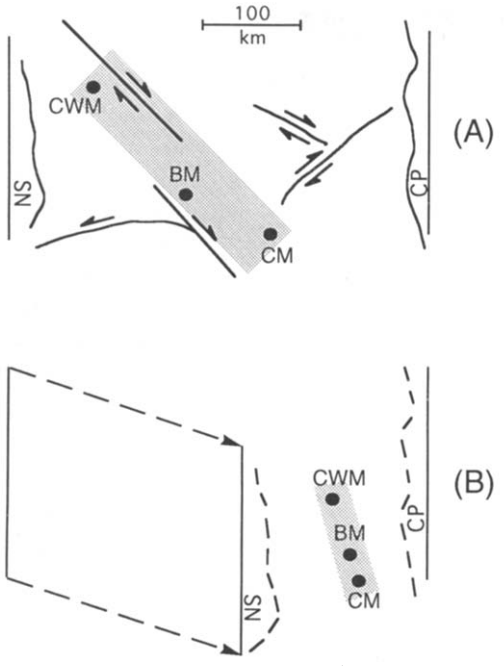

Fig. 5. Localities of surface exposures of Permian to Triassic plutons (*CWM* and *CM*) and cooling ages (*BM*) in the Death Valley region. (A) Present-day localities. (B) Pre-extensional localities (after Snow [30]). *SN* = Sierra Nevada; *CP* = Colorado Plateau; *CWM* = Cottonwood Mountains; *CM* = Clark Mountains; *BM* = Black Mountains. See text for discussion.

roofing. This contrasts with samples DKH–IH2 and DKH–JP which experienced middle Miocene cooling from above 200°C to below 100°C (Table 4 and Fig. 4b).

Central Black Mountains Core: Figures 4c–e depict cooling path envelopes constructed for samples from the crystalline core of the Black Mountains. Figure 4c represents temperature–age data obtained from the Willow Spring Pluton collected at Gold Valley (sample 988–25) and Figs. 4d and e represent data from Precambrian basement sampled from the Copper Canyon turtleback (sample 89–CC) and the Mormon Point turtleback (sample 89–MP). The $^{40}Ar/^{39}Ar$ hornblende age for sample 89–CC shows a diffusion-loss gradient with a low-temperature age minimum of 11.8 Ma and a high-temperature maximum of 14.5 Ma. This spectrum has been interpreted to represent partial resetting by the 11.6 Ma Willow Spring Pluton whereas the 10 Ma plateau hornblende age from sample 89–MP was interpreted as a completely reset age [10].

It is important to note that the width of the cooling path envelope created by the relatively low precision of the fission-track ages is greatly reduced for some of the samples when interpreted together with the $^{40}Ar/^{39}Ar$ ages. This is a consequence of the fact that the cooling path envelope cannot have a negative slope (i.e., any particular cooling path cannot progress to older ages with time). This is best exemplified by Fig. 4d. Although the zircon fission-track age is 8.0 ± 1.9 Ma, the 6.7 ± 0.1 Ma biotite age provides a realistic upper age limit of 6.8 Ma. Therefore, this sample is constrained to have cooled from above ~ 300°C to below ~ 200°C between 6.8 and 6.1 Ma, indicating a rapid cooling rate of > 150°C/Ma.

Northern Black Mountains: Figure 4f depicts the cooling history of rocks making up the Badwater turtleback. The 24 Ma muscovite and ~ 13 Ma biotite $^{40}Ar/^{39}Ar$ ages suggest that these rocks cooled slowly (< 5°C/Ma) prior to the onset of intrusion and unroofing of the range block beginning at 11–12 Ma. The zircon fission-track age implies an increase in the rate of cooling after 13 Ma (from < 5°C/Ma to 15–50°C/Ma). Fine-grained dioritic dikes intruded the Badwater turtleback at 6.3 Ma [10], concurrent with brittle faulting [42].

Greenwater Range: A Tertiary granite exposed in the southern Greenwater range (Fig. 2) yielded a 9.8 ± 0.1 Ma $^{40}Ar/^{39}Ar$ biotite plateau age and a 7.7 ± 1.7 Ma zircon fission-track age. This granite has been interpreted by Holm et al. [10] as a shallow-level granite intruded at ~ 10 Ma. It is unconformably overlain by 8.5–7.5 Ma volcanic rocks [20], suggesting that it was unroofed shortly after intrusion.

Ashford Canyon: The oldest cooling ages in the Black Mountains have been obtained from Precambrian basement samples collected from the vicinity of Ashford canyon beneath the depositional contact with Upper Precambrian strata (Fig. 2, [26]). A muscovite $^{40}Ar/^{39}Ar$ age of ~ 1.4 Ga was obtained from micaschist (sample AM–UNC–M) directly beneath the nonconformity south of Ashford Canyon (Table 4). A sample of Precambrian basement from north of the canyon (AM2a–M) yielded a $^{40}Ar/^{39}Ar$ total gas age of 283 ± 4 Ma and a zircon fission-track age of 18.9 ± 3.2 Ma.

7. Discussion

7.1 Timing of unroofing

Discordant mica $^{40}Ar/^{39}Ar$ ages from Precambrian basement rocks of the Badwater turtleback suggest little unroofing prior to the onset of intrusion [10]. Relative tectonic quiescence prior to the onset of major extension has been suggested for this region based on the sedimentologic record northeast of the Badwater turtleback [43]. Apatite and zircon ages from the southeastern Black Mountains and the Greenwater Range suggest that major unroofing and tilting occurred here at ~ 13–8.5 Ma. We interpret the 15.2 Ma zircon age of sample DKH–IH2 as a mixed age due to its being in the zone of partial annealing for zircon prior to unroofing. (Note its proximity to sample DKH–IH1, which was located above the zone of partial annealing for zircon prior to Miocene unroofing.)

Cooling ages from the central Black Mountains are younger than those obtained from the southeastern Black Mountains, suggesting that unroofing occurred later there. For example, zircon fission-track ages of ~ 6–9 Ma occur north of the Amargosa chaos, whereas zircon ages to the south range from ~ 11 to > 90 Ma. In addition, minerals with higher closure temperatures yielded late Miocene ages concordant with ages obtained from minerals with lower closure temperatures. The young biotite $^{40}Ar/^{39}Ar$ ages from both the Willow Spring Pluton and subjacent basement rocks in this area indicate rapid cooling from above 300°C. These data suggest that rocks from the central Black Mountains cooled both later (at ~ 8.5–6.0 Ma vs. ~ 13–9.0 Ma) and from higher temperatures than did rocks from the southeastern Black Mountains.

Apatite fission-track ages from the crystalline core of the range suggest that rapid unroofing brought these rocks to within a few kilometers of the earth's surface and that there has been little cooling and associated unroofing of the Death Valley antiforms since about 6–5 Ma. Although the Black Mountains escarpment has continued to be active, it is likely that no more than 3–4 km of unroofing, and probably less than this, occurred over the past 5 m.y. or so.

7.2 Depth of unroofing

Holm et al. [10] proposed that the Willow Spring Pluton intruded into country rock with temperatures above 300°C. As the central Death Valley region was relatively amagmatic for 10 m.y. prior to intrusion, it seems probable that the geotherm was neither greatly disturbed nor inordinantly high when the pluton intruded. Fitzgerald et al. [44] reported old pre-extensional apatite cooling ages at a structural depth of 4.5 km beneath the Tertiary unconformity in the Gold Butte block of southeastern Nevada. This suggests that the average upper crustal geothermal gradient at this latitude in Miocene time was probably between 20 and 25°C/km and probably

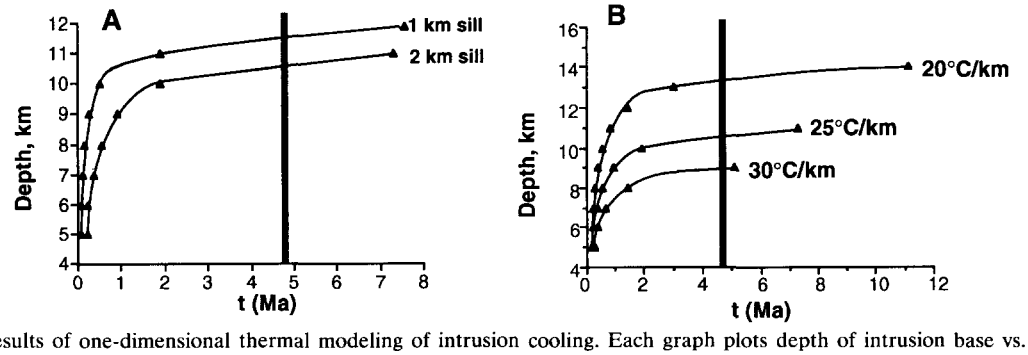

Fig. 6. Results of one-dimensional thermal modeling of intrusion cooling. Each graph plots depth of intrusion base vs. the time after crystallization at which the base of a sill-shaped pluton will cool through 300°C. The vertical line at 4.7 Ma represents the time after crystallization at which the base of the Willow Spring Pluton cooled through 300°C. (A) Results of modeling assuming an average geothermal gradient of 25°C/km prior to intrusion and pluton thicknesses of 1 and 2 km. (B) Results of thermal modeling assuming a 2 km thick pluton and variable geothermal gradients of 20, 25 and 30°C/km prior to intrusion. See appendix.

no greater than 30°C/km. This is consistent with a relatively normal pre-extensional geotherm throughout much of the Basin and Range Province [45], and with a rising average geothermal gradient associated with extension since Miocene time and reaching about 30°C/km at present [46]. Considering an upper bound for the average geothermal gradient of 30°C/km prior to intrusion of the Willow Spring Pluton gives a minimum depth of emplacement of 10 km. This minimum is consistent with two independent results from the Al-in-hornblende geobarometer that suggest a minimum intrusion depth of 9–12 km [28,47].

The cooling history of the Willow Spring Pluton can also serve as an independent measure of the depth of intrusion. Time-governing equations for thermal decay of a pluton [48] indicate that its temperature will rapidly approach the temperature of the country rock in the first 1–2 m.y. after crystallization. Figure 6 shows the results of one-dimensional modeling for thermal decay of a sill-like intrusion (see appendix). The graphs show the time after crystallization at which the base of the intrusion would cool through 300°C for variable depths. In our modeling we have assumed a standard thermal diffusivity of 10^{-6} m^2/s, a crystallization temperature of 900°C ± 100°C, and geothermal gradients between 20 and 30°C/km. While there is always some degree of uncertainty in the estimation of these parameters, we consider the limits chosen to be within two standard deviations of the actual values. The results are relatively insensitive to crystallization temperature (e.g., choosing an initial temperature of 1000°C typically changes the depth estimate by less than 0.15 km). The pluton is exposed over a vertical relief above its base of about 1 km. We consider this a likely intrusion thickness but we allow for twice that thickness in our thermal modeling. Biotite $^{40}Ar/^{39}Ar$ cooling ages at and near the base of the intrusion indicate the pluton cooled through 300°C about 4.7 Ma after crystallization [10]. If we consider the biotite ages to represent cooling simply due to loss of intrusion heat, the results from thermal modeling (Fig. 6a and b) show that the base of the pluton would have intruded at a likely depth of 11.1 ± 2.5 km (using an approximation for the standard deviation; Bevington [49], eq. 4–9). This estimate would represent a minimum depth as the modeling assumes the base of the pluton remained stationary throughout its cooling. Unroofing during that time would cause cooling to be accelerated and thus require greater depths for emplacement.

7.3 Tectonic implications

A fundamental consequence of normal faulting is that deeper (warmer) crustal levels are brought nearer to the surface and juxtaposed with shallower (colder) crustal levels. Following the second law of thermodynamics, foot wall rocks rapidly cool toward equilibration with the hanging wall. Also, as unroofing rates for tectonic denudation are generally rapid, rocks unroofed by normal faulting will normally cool more quickly than rocks unroofed by erosion-dominated processes [50,51].

The actual cooling histories reconstructed here compare well with the generalized cooling history expected for westerly directed tectonic denudation. The cooling path envelopes show slow cooling at relatively high temperatures followed by rapid cooling which we associate with tectonic denudation (Fig. 4). The cooling histories suggest a migration of rapid cooling across the range block during the time span ~ 12–6 Ma. The diachroneity and rapid rate of cooling, as well as cooling from progressively warmer temperatures toward the northwest, all seem to suggest that unroofing occurred by tectonic denudation rather than by erosion-dominated processes. The morphology of the cooling path envelopes constructed here is similar to those constructed for other detachment fault terranes. We conclude that cooling of rocks in the Black Mountains probably reflects large-scale tectonic denudation similar to that observed for other metamorphic core complexes [4,36,52–57].

Analysis of the age and correlation of Miocene volcanic rocks in this region also argues against an erosion-dominated process. Volcanic strata of ca. 11 Ma and younger on the eastern portion of the Panamint Range (Fig. 7) have been correlated with volcanic rocks on the southeastern portion of the Black Mountains [26,58]. This suggests either that (1) the area between (currently occupied by the crystalline rocks of the Black Mountains) was a site of basin development and

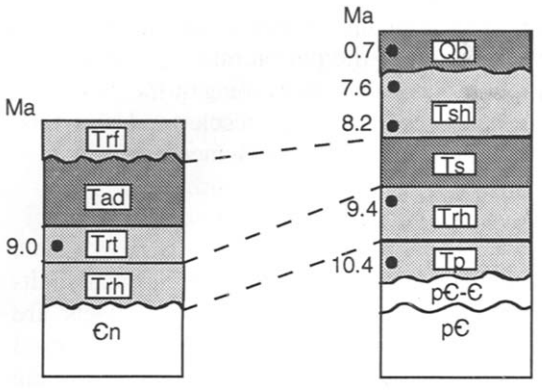

Fig. 7. Generalized stratigraphic columns showing correlated units in the eastern Panamint Range and the Black Mountains. Ages (K-Ar) are from Wright and Troxel [26] and Hildreth [unpublished]. *Trf* = rhyolite flow; *Tad* = basaltic andesite; *Trt* = rhyolite tuff; *Trh* = lithic ash-flow tuff (Rhodes tuff in Black Mountains); *Cn* = Nopah Formation; *Qb* = basalt of Cinder Cone Hill; *Tsh* = Shoshone volcanics; *Ts* = Sheephead andesite; *Tp* = pre-Rhodes volcanic units; *pC–C* = unmetamorphosed Late Precambrian–Cambrian strata; *pC* = Precambrian basement ± metamorphosed Late Proterozoic cover.

areally extensive volcanic accumulation or (2) the volcanic rocks in the Panamint Range were tectonically transported away from their initial position east of the Black Mountains. Both of these possibilities preclude late Miocene (12–6 Ma) unroofing by erosion of the miogeoclinal section. It seems reasonable to conclude that volcanic accumulation occurred simultaneously with detachment faulting and associated tectonic unroofing of the Black Mountains and that the volcanic rocks are detached strata brought to rest on the crystalline complex during tectonic denudation.

Figure 8 is a summary plot of mean cooling-age data (micas, sphene, zircon and apatite) from the Black Mountains projected onto a NW-oriented section beginning below the Precambrian nonconformity in the southeastern portion of the range and extending to the northern end of the Copper Canyon turtleback (line A–A' of Fig. 2). Excluding the data obtained from just beneath the Amargosa chaos rocks, mineral ages decrease towards the northwest with increasing distance away from the nonconformity. The old cooling ages from the Ashford Canyon region are consistent with the notion that these rocks are part of an allochthonous slice [6]. Holm and Wernicke [28] interpreted these rocks (and the overlying strata which constitute the Amargosa chaos) to have been translated 15–20 km northwestward away from their initial position in the southeastern Black Mountains. According to their interpretation, these rocks would represent a stranded portion of the hanging wall left behind as a highly distended and fault-bounded rock mass. This interpretation implies that the oldest cooling ages should be obtained from the Ashford Canyon area and that cooling ages would decrease towards the northwest away from the Precambrian nonconformity (Fig. 8).

The monotonically decreasing cooling ages from mineral thermochronometers across the central core of the range block suggest that unroofing occurred along a single major gently dipping detachment zone [10]. Unroofing by a combination of erosion and high-angle normal faulting throughout the range [23] seems difficult to reconcile with this pattern of cooling. Rather, the entire range block represents a relatively intact

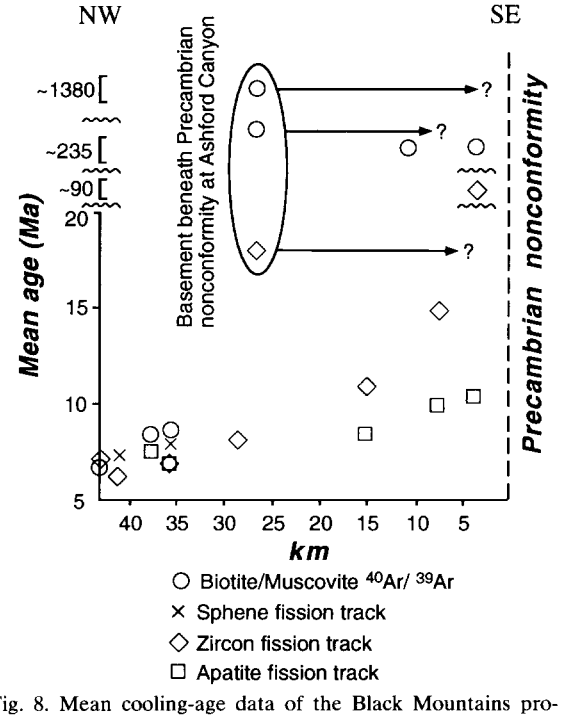

Fig. 8. Mean cooling-age data of the Black Mountains projected onto a NW-trending cross section (A–A' of Fig. 2). See text for discussion.

NW-deepening section of the pre-extensional crust unroofed during Neogene extension. Mica ages from the Badwater turtleback (Table 4) indicate that these rocks were at a shallower depth prior to extension than rocks making up the two southern turtlebacks. Holm et al. [10] interpreted these rocks as either having been displaced towards the northwest, perhaps along a mid-crustal splay of the detachment zone in similar fashion to the rocks of the Amargosa chaos, or as occurring along a NW-trending ramp of the detachment.

7.4 Mechanical model of extension

The reconstruction of cooling histories suggests that cooling occurred rapidly in specific regions and that it migrated towards the northwest. We interpret this pattern of cooling as a result of the lower plate undergoing major flexural deformation as it pulls out from underneath a relatively rigid, scoop-shaped hanging wall block. This model for extensional deformation (the 'rolling hinge' model) has been proposed previously for this region and elsewhere [59–62]. However, to our knowledge, this is the first study which documents a pattern of foot wall cooling and unroofing within a single range block which appears to support this model.

This migration of unroofing and tilting within the range mimics the overall east to west sequential tilting of range blocks at this latitude [29,63]. The timing constraints presented here support a model of sequential detachment of range-scale blocks away from the trailing edge of a westward migrating crustal block [59,62]. Similar thermochronologic evidence for sequential range-scale tilting has been obtained from the Lake Mead extended region [44], suggesting that this style of extension might provide an explanation for strongly extended domains in the Basin and Range in general.

The results of this study suggest that the deepest portions of foot wall rocks were tectonically unroofed from temperatures in the 300–400°C range at depths of 10–15 km. Recent thermochronologic studies of exposed foot wall rocks both north (Funeral Mountains) and south (Mojave Extensional Belt) of the Black Mountains have yielded similar results with rapid unroofing of rocks from temperatures between 300–350°C [36,64]. The now moderately to steeply tilted stratified rocks at upper crustal levels, and steep fault–bed angles, suggest that the detachment faults in these areas initially dipped more steeply through the upper crust [60,65–67]. However, the great distances of exposed foot wall relative to the amount of unroofing suggested by the moderate, pre-extensional temperatures of the deepest portions seem to require more gentle dips of the detachment in the middle crust. The 300–350°C temperatures associated with the lower dips generally correspond to the onset of crystal–plastic deformation mechanisms in quartzose rocks. It thus seems likely that, at least in this region, the flattening of crustal scale listric detachment faults corresponds to a rheological transition from cataclastic to crystal–plastic deformation mechanisms as hypothesized by a number of earlier workers [68–70].

Acknowledgements

This work was supported by a National Science Foundation grant (EAR-9004821) awarded to Stein Jacobsen and Brian Wernicke. We thank Stein Jacobsen, Jane Selverstone, Brian Wernicke and Lauren Wright for very helpful comments and Terry Pavlis for a thorough and thoughtful review. Sara Holm and Pete George assisted in the field and laboratory. We are grateful to the National Park Service for allowing field work and sampling in the Black Mountains.

Appendix

The time-governing equation for thermal decay of the base of a sill through a specified temperature is given by:

$$T_S = \frac{[T_b + (x+a)G]}{2}\left[\mathrm{erf}\left[(2a)/(2\sqrt{\alpha t})\right]\right] + (x+a)G$$

where T_s = specified temperature, T_b = crystallization temper-

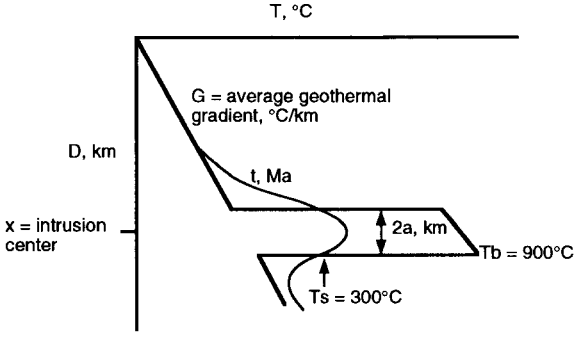

ature at the pluton base, x = depth of the center of the sill, a = sill half-thickness, a is the thermal diffusivity, G = geothermal gradient and t = time after crystallization (modified [48]). We specify $T_s = 300°C$ and consider $\alpha \approx 10^{-6}$ m^2/s. Solving for $x + a$ gives:

$$x + a = 300 - (T_b/2)\left\{\text{erf}\left[(a)/(5\sqrt{t})\right]\right\}/ G\left\{1/2\left[\text{erf}\left[(a)/(5\sqrt{t})\right]\right]+1\right\}$$

We consider $T_b = 900 \pm 100°C$. For the Willow Spring Pluton in the Black Mountains, $t = 4.7$ Ma, $a = 0.5$–1.0 km and $G = 20$–$30°C$/km.

References

1 I. McDougall and T.M. Harrison, Geochronology and Thermochronology by the $^{40}Ar/^{39}Ar$ Method, Oxford University Press, New York, 1988.

2 T.M. Harrison, R.L. Armstrong, C.W. Naeser and J.E. Harakal, Geochronology and thermal history of the Coast Plutonic Complex, near Prince Rupert, British Columbia, Can. J. Earth Sci. 16, 400–410, 1979.

3 P.K. Zeitler, N.M. Johnson, C.W. Naeser and R.A.K. Tahirkheli, Fission-track evidence for Quaternary uplift of the Nanga Parbat region, Pakistan, Nature 298, 255–257, 1982.

4 R.K. Dokka, M.J. Mahaffie and A.W. Snoke, Thermochronologic evidence of major tectonic denudation associated with detachment faulting, northern Ruby Mountains–east Humboldt Range, Nevada, Tectonics 5, 995–1006, 1986.

5 J.H. Stewart, Extensional tectonics in the Death Valley area, California: Transport of the Panamint Range structural block 80 km northwestward, Geology 11, 153–157, 1983.

6 L.F. Noble, Structural features of the Virgin Spring area, Death Valley, California, Geol. Soc. Am. Bull. 52, 941–1000, 1941.

7 H. Drewes, Geology of the Funeral Peak quadrangle, California, on the eastern flank of Death Valley, U.S. Geol. Surv. Prof. Pap. 413, 78 pp., 1963.

8 J.K. Otton, Geology of the central Black Mountains, Death Valley, California: The Turtleback terrane, 155 pp., Ph.D. Thesis, Pennsylvania State Univ., 1977.

9 Y. Asmerom, J.K. Snow, D.K. Holm, S.B. Jacobsen, B.P. Wernicke and D.R. Lux, Rapid uplift and crustal growth in extensional environments: An isotopic study from the Death Valley region, California, Geology 18, 223–226, 1990.

10 D.K. Holm, J.K. Snow and D.R. Lux, Thermal and barometric constraints on the intrusion and unroofing history of the Black Mountains: Implications for timing, initial dip, and kinematics of detachment faulting in the Death Valley region, CA, Tectonics 11, 507–522 1992.

11 L.A. Wright, J.K. Otton and B.W. Troxel, Turtleback surfaces of Death Valley viewed as phenomena of extension, Geology 2, 53–54, 1974.

12 D.K. Holm and D.R. Lux, The Copper Canyon Formation: A record of unroofing and Tertiary folding of the Death Valley Turtleback surfaces, Geol. Soc. Am. Abstr. Programs 23, 35, 1991.

13 T.L. Pavlis, Exposures of the floor of a Miocene, syntectonic pluton, Death Valley, California: the turtleback terrane, Geol. Soc. Am. Abstr. Progams 23, A189, 1991.

14 R.J. Fleck, Age and tectonic significance of volcanic rocks, Death Valley area, California, Geol. Soc. Am. Bull. 81, 2807–2816, 1970.

15 P.J. Scrivner, Stratigraphy, sedimentology, and vertebrate ichnology of the Copper Canyon Formation (Neogene), Death Valley National Monument, 134 pp., M.S. Thesis, Univ. Southern California, 1984.

16 L.A. Wright and B.W. Troxel, Shallow-fault interpretation of Basin and Range structure, southwestern Great Basin, in: Gravity and Tectonics, K.A. DeJong and R. Scholten, eds., pp. 397–407, Wiley, New York, 1973.

17 A.R. Prave and L.A. Wright, Isopach pattern of the Lower Cambrian Zabriskie Quartzite, Death Valley region, California–Nevada: How useful in tectonic reconstructions?, Geology 14, 251–254, 1986.

18 A.R. Prave and L.A. Wright, Reply to Comment on "Isopach pattern of the Lower Cambrian Zabriskie Quartzite, Death Valley region, California–Nevada: How useful in tectonic reconstructions?", Geology 14, 811–812, 1986.

19 I. Cemen and L.A. Wright, Neogene conglomerates of the Furnace Creek basin, Death Valley California: origin and tectonic significance, Geol. Soc. Am. Abstr. Progams 23, A82, 1991.

20 L.A. Wright and eight others, Cenozoic magmatic and tectonic evolution of the east-central Death Valley region, California, Geol. Soc. Am. Annu. Meet. Guideb., San Diego, Calif., pp. 93–127, 1991.

21 L.A. Wright, M. Ellis, B. Troxel and R. Thompson, Neogene and active tectonic development of the Death Valley–Resting Springs pull-apart, Eos Trans. AGU 72, 461, 1991.

22 L.A. Wright, Overview of the role of strike-slip and normal faulting in the Neogene history of the region northeast of Death Valley, California–Nevada, in: Late Cenozoic Evolution of the Southern Great Basin, Open File 89-1, M.A. Ellis, ed., pp. 1–12, Nev. Bur. Mines Geol., Reno, 1989.

23 G. King and M. Ellis, The origin of large local uplift in extensional regions, Nature 348, 689–693, 1990.

24 M.G. Miller, High-angle origin of the currently low-angle Badwater Turtleback fault, Death Valley, California, Geology 19, 372–375, 1991.

25 L.A. Wright, L. Serpa and B.W. Troxel, Tectono-chronologic model for wrench fault related crustal extension, Death Valley area, California, Geol. Soc. Am. Abstr. Programs 19, 898–899, 1987.

26 L.A. Wright and B.W. Troxel, Geology of the northern half of the Confidence Hills 15′ quadrangle, Death Valley region, eastern California: The area of the Amargosa chaos, Calif. Div. Mines Geol. Map Sheet 34, Scale 1:24,000, 1984.

27 C.B. Hunt and D.R. Mabey, Stratigraphy and structure, Death Valley, California, U.S. Geol. Surv. Prof. Pap. 494-A, 162 pp., 1966.

28 D.K. Holm and B. Wernicke, Black Mountains crustal

section, Death Valley extended terrain, California, Geology 18, 520–523, 1990.
29 B. Wernicke, G.J. Axen and J.K. Snow, Basin and Range extensional tectonics at the latitude of Las Vegas, Nevada, Geol. Soc. Am. Bull. 100, 1738–1757, 1988.
30 J.K. Snow, Cordilleran orogenesis, extensional tectonics and geology of the Cottonwood Mountains area, Death Valley region, California and Nevada, Ph.D. Thesis, Harvard Univ., 1990.
31 M.C. Johnson and M.J. Rutherford, Experimental calibration of the aluminum-in-hornblende geobarometer with application to Long Valley caldera (California) volcanic rocks, Geology 17, 837–841, 1989.
32 L.S. Hollister, G.C. Grissom, E.K. Peters, H.H. Stowell and V.B. Sisson, Confirmation of the empirical correlation of Al in hornblende with pressure of solidification of calc-alkaline plutons, Am. Mineral. 72, 231–239, 1987.
33 C.W. Naeser, Fission-track dating, U.S. Geol. Surv. Open File Rep. 76-190, 1–65, 1976.
34 R.F. Galbraith, On statistical models for fission track counts, J. Math. Geol. 13, 471–478, 1981.
35 M.H. Dodson, Closure temperature in cooling geochronological and petrological systems, Contrib. Mineral. Petrol. 40, 259–274, 1973.
36 D.K. Holm and R.K. Dokka, Major late Miocene cooling of the middle crust associated with extensional orogenesis in the Funeral Mountains, California, Geophys. Res. Lett. 18, 1775–1778, 1991.
37 J.F. Sutter, Geochronology of major thrusts, southern Great Basin, California, M.A. Thesis, Rice Univ., 1968 (Unpubl.).
38 B.C. Burchfiel and G.A. Davis, Clark Mountain thrust complex in the Cordillera of southeastern California: geologic summary and field trip guide, Calif. Univ. Riverside Campus Mus. Contrib. 1, 1–28, 1971.
39 J.K. Snow, Y. Asmerom and D.R. Lux, Permian–Triassic plutonism and tectonics, Death Valley region, California and Nevada, Geology 19, 629–632, 1991.
40 J.K. Snow, Large-magnitude Permian shortening and continental-margin tectonics in the southern Cordillera, Geol. Soc. Am. Bull. 104, 80–105, 1992.
41 J.K. Snow and B. Wernicke, Uniqueness of geological correlations: An example from the Death Valley extended terrain, Geol. Soc. Am. Bull. 101, 1351–1362, 1989.
42 M.G. Miller, The Badwater turtleback fault, Black Mountains, Death Valley, CA: Its geometry and lower plate deformation, Geol. Soc. Am. Abstr. Programs 22, 68–69, 1990.
43 I. Cemen and L.A. Wright, Cenozoic extension in northern Death Valley: evidence from the sedimentary rocks surrounding the Funeral Mountains, Geol. Soc. Am. Abstr. Programs 20, 149, 1988.
44 P.G. Fitzgerald, J.E. Fryxell and B.P. Wernicke, Miocene crustal extension and uplift in southeastern Nevada: Constraints from fission track analysis, Geology 19, 1013–1016, 1991.
45 T.A. Dumitru, P.B. Gans, D.A. Foster and E.L. Miller, Refrigeration of the western Cordilleran lithosphere during Laramide shallow-angle subduction, Geology 19, 1145–1148, 1991.
46 A.H. Lachenbruch and J.H. Sass, Models of an extending lithosphere and heat flow in the Basin and Range province, in: Cenozoic Tectonics and Regional Geophysics of the Western Cordillera, R.B. Smith and G.P. Eaton, eds., Geol. Soc. Am. Mem. 152, 209–250, 1978.
47 K.J. Meurer and T. Pavlis, Evolution of the Black Mountain crustal block, Death Valley, California: Two component rotation during Neogene extension, Eos Trans. AGU 72, 469–470, 1991.
48 H.S. Carslaw and Jaegar, J.C., Conduction of Heat in Solids, 2nd ed., 510 pp., Oxford University Press, 1959.
49 P.R. Bevington, Data Reduction and Error Analysis for the Physical Sciences, McGraw-Hill, 1969.
50 C. Ruppel, L. Royden and K. Hodges, Thermal modeling of extensional tectonics: application to the pressure-temperature-time histories of metamorphic rocks, Tectonics 7, 947–957, 1988.
51 W.R. Buck, F. Martinez, M.S. Steckler and J.R. Cochran, Thermal consequences of lithospheric extension: pure and simple, Tectonics 7, 213–234, 1988.
52 R.D. Dallmeyer, A.W. Snoke and E.H. McKee, The Mesozoic–Cenozoic tectonothermal evolution of the Ruby Mountains, East Humbolt Range, Nevada, Tectonics 6, 931–954, 1986.
53 E. DeWitt, J.F. Sutter, G.A. Davis and J.L. Anderson, ^{40}Ar–^{39}Ar age-spectrum dating of Miocene mylonitic rocks, Whipple Mountains, southeastern California, Geol. Soc. Am. Abstr. Programs 18, 584, 1986.
54 R.K. Dokka and S.H. Lingrey, Fission track evidence for a Miocene cooling event, Whipple Mountains, southeastern California, in: Cenozoic Paleogeography of the Western United States, J.M. Armentrout et al., eds., pp. 141–146, Pac. Sect., Soc. Econ. Paleontol. Mineral., Los Angeles, Calif., 1979.
55 R.K. Dokka and ten others, Aspects of the Mesozoic and Cenozoic Geologic Evolution of the Mojave Desert: Guidebook of the Geological Society of America Annual Meeting, San Diego, California, pp. 1–43, 1991.
56 D.A. Foster, T.M. Harrison, C.F. Miller and K.A. Howard, The $^{40}Ar/^{39}Ar$ thermochronlogy of the eastern Mojave Desert, California, and adjacent western Arizona with implications for the evolution of metamorphic core complexes, J. Geophys. Res. 95, 20,005–20,024, 1990.
57 S.M. Richard, J.E. Fryxell and J.F. Sutter, Tertiary structure and thermal history of the Harquahala and Buckskin Mountains, west-central Arizona: Implications for denudation by a major detachment fault system, J. Geophy. Res. 95, 19,973–19,989, 1990.
58 L.W. McKenna and K.V. Hodges, Constraints on the kinematics and timing of late Miocene–Recent extension between the Panamint and Black Mountains, southeastern California, in: Basin and Range Extensional Tectonics near the Latitude of Las Vegas, Nevada, B.P. Wernicke, ed., Geol. Soc. Am. Mem. 176, 363–376, 1991.
59 W.R. Buck, Flexural rotation of normal faults, Tectonics 7, 959–973, 1988.
60 W.B. Hamilton, Detachment faulting in the Death Valley region, California and Nevada, U.S. Geol. Surv. Bull. 1790, 51–85, 1988.
61 J.E. Spencer and S.J. Reynolds, Tectonics of mid-Tertiary

extension along a transect through west central Arizona, Tectonics 10, 1204–1221, 1991.
62 B. Wernicke and G.J. Axen, On the role of isostasy in the evolution of normal fault systems, Geology 16, 848–851, 1988.
63 L.A. Wright, R.E. Drake and B.W. Troxel, Evidence for westward migration of severe Cenozoic extension, southeastern Great Basin, California, Geol. Soc. Am. Abstr. Programs 16, 701, 1984.
64 D.J. Henry and R.K. Dokka, Metamorphic evolution of exhumed middle to lower crustal rocks in the Mojave Extensional Belt, southern California, U.S.A., J. Metamorph. Geol. 10, 347–364, 1992.
65 D.K. Holm, Initial dip, geometry, and kinematics of detachment faulting in the Death Valley region, CA, Geol. Soc. Am. Abstr. Programs 23, A189, 1991.
66 B.P. Wernicke, Low-angle faults in the Basin and Range Province: Nappe tectonics in an extending orogen, Nature 291, 645–648, 1981.
67 B.P. Wernicke, Uniform-sense normal simple shear of the continental lithosphere, Can. J. Earth Sci. 22, 108–125, 1985.
68 B. Wernicke, Rheological stratification of the crust during Cordilleran extension: The brittle–plastic and plastic–fluid transition zones, Geol. Soc. Am. Abstr. Programs 23, A190, 1991.
69 G.S. Lister and G.A. Davis, The origin of metamorphic core complexes and detachment faults formed during Tertiary continental extension in the northern Colorado River region, U.S.A., J. Struct. Geol. 11, 65–94, 1989.
70 R.K. Dokka and R.H. Pilger, A non-uniform extension model for continental rifting, Geol. Soc. Am. Abstr. Programs 15, 559, 1983.
71 R. Streitz and M.C. Stinson, Compilers, Death Valley sheet, in: The Collection Geologic map of California, Calif. Div. Mines Geol., Sacramento, Scale 1:250,000, 1974.
72 P.F. Green, A new look at statistics in fission track dating, Nucl. Tracks 5, 77–86, 1981.